The wave of first spikes provides robust spatial cues for retinal information processing

Geoffrey Portelli, John Barrett, Evelyne Sernagor, Timothée Masquelier, Pierre Kornprobst

The wave of first spikes provides robust spatial cues for retinal information processing

Geoffrey Portelli, John Barrett, Evelyne Sernagor, Timothée Masquelier, Pierre Kornprobst

RESEARCH REPORT

N° 8559

July 2014

Project-Team Neuromathcomp

ISSN 0249-6399 ISRN INRIA/RR--8559--FR+ENG

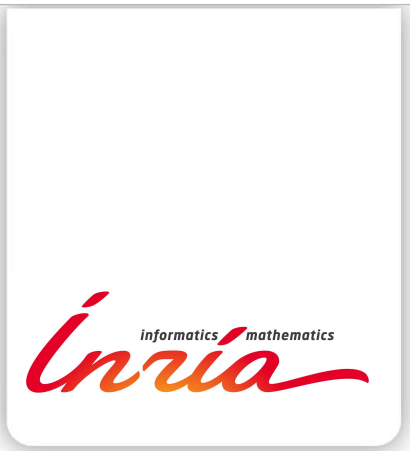

The wave of first spikes provides robust spatial cues for retinal information processing

Geoffrey Portelli*, John Barrett†, Evelyne Sernagor†, Timothée Masquelier‡§, Pierre Kornprobst*

Project-Team Neuromathcomp

Research Report n° 8559 — July 2014 — 19 pages

* Neuromathcomp Project Team, Inria Sophia Antipolis - Méditerranée, France
† Institute of Neuroscience, Newcastle, UK
‡ Institut de la Vision, UPMC Université Paris 06, Paris, France
§ CNRS, UMR 7210, Paris, France

RESEARCH CENTRE
SOPHIA ANTIPOLIS – MÉDITERRANÉE

2004 route des Lucioles - BP 93
06902 Sophia Antipolis Cedex

Abstract: How a population of retinal ganglion cells (RGCs) encode the visual scene remains an open question. Several coding strategies have been investigated out of which two main views have emerged: considering RGCs as independent encoders or as synergistic encoders, i.e. when the concerted spiking in a RGC population carries more information than the sum of the information contained in the spiking of individual RGCs. Although the RGCs assumed as independent encode the main information, there is currently a growing body of evidence that considering RGCs as synergistic encoders provides complementary and more precise information. Based on salamander retina recordings, it has been suggested [11] that a code based on differential spike latencies between RGC pairs could be a powerful mechanism. Here, we have tested this hypothesis in the mammalian retina. We recorded responses to stationary gratings from 469 RGCs in 5 mouse retinas. Interestingly, we did not find any RGC pairs exhibiting clear latency correlations (presumably due to the presence of spontaneous activity), showing that individual RGC pairs do not provide sufficient information in our conditions. However considering the whole RGC population, we show that the shape of the wave of first spikes (WFS) successfully encodes for spatial cues. To quantify its coding capabilities, we performed a discrimination task and we showed that the WFS was more robust to the spontaneous firing than the absolute latencies are. We also investigated the impact of a post-processing neural layer. The recorded spikes were fed into an artificial lateral geniculate nucleus (LGN) layer. We found that the WFS is not only preserved but even refined through the LGN-like layer, while classical independent coding strategies become impaired. These findings suggest that even at the level of the retina, the WFS provides a reliable strategy to encode spatial cues.

Key-words: retina, latency, neural coding, rank order coding, concerted spiking pattern

La première vague de potentiels d'action encode des indices spatiaux pour le traitement de l'information rétinienne

Résumé : Comment une population de cellules ganglionnaires de la rétine (RGC) encode la scène visuelle reste une question ouverte. Plusieurs stratégies de codage ont été étudiés à partir desquelles deux principales vues ont émergé: considérer les RGCs en tant que encodeurs indépendants ou en tant que encodeurs synergique; c'est à dire lorsque la réponse concertée dans une population de RGCs contient plus d'informations que la somme des informations contenues dans les réponses individuelles. Bien que en considérant les RGCs comme des encodeurs indépendants donne accès à l'information principale, il existe actuellement un nombre croissant de preuves qui montrent que considérer les RGCs comme des encodeurs synergiques fournit des informations complémentaires et plus précises. Basé sur des enregistrements de la rétine de salamandre, il a été suggéré [11] qu'un code basé sur les différences entre les latences des paires de RGCs pourrait être un mécanisme puissant. Ici, nous avons testé cette hypothèse dans la rétine de mammifère. Nous avons enregistré les réponses de 469 RGCs de 5 rétines de souris. Fait intéressant, nous n'avons pas trouvé de paires de RGCs présentant des corrélations de latence claires (probablement en raison de la présence d'une forte activité spontanée). Cela montre que les paires de RGCs individuelles ne fournissent pas suffisamment d'informations dans nos conditions. Toutefois, en considérant la population de RGCs, nous avons montré que la forme de la première vague de potentiels d'action (WFS) code avec succès des indices spatiaux. Pour quantifier ses capacités de codage, nous avons réalisé une tâche de discrimination et nous avons montré que la WFS était plus robuste à l'activitée spontannée que les latences absolues. Nous avons également étudié l'impact du traitement par une couche de neurones. Les réponses enregistrées ont été introduits dans une couche de corps géniculé latéral artificiel (LGN). Nous avons constaté que la WFS est non seulement préservée mais mÃªme raffinée à travers la couche LGN, tandis que les stratégies classiques de codage indépendant deviennent altérées. Ces résultats suggèrent que, même au niveau de la rétine, la WFS propose une stratégie fiable pour coder l'information visuelle.

Mots-clés : rétine, latence, code neural, rank order code, codage de population

1 Introduction

Understanding information processing in the nervous system by exploring the neural code is a current challenge in the neuroscience community. Different quantitative methods have been proposed and it has been possible to decipher how some neural systems encode and process information [30]. However as far as the retina is concerned, many questions remain open about how spike trains generated by retinal ganglion cells (RGC) encode the wealth of information about the visual environment. Several coding strategies have been investigated using mostly artificial stimuli. Two main streams of thought have emerged: one that considers RGCs as independent encoders, and one that considers them as synergistic encoders.

Several studies have shown which information can be extracted from RGC responses when considering them as independent encoders. For example, in [12] the authors showed that information can be read out from simple response features such as the spike count or latency of the first spike event or from latency between the different spike events. More complex features can also be considered as proposed in [17] when doing a visual discrimination task experiment in mouse both *in vivo* and *in vitro*. The authors showed that simple coding strategies such as spike count coding are insufficient to replicate behavioral performances. More information-rich codes such as spike timing that take into account time correlations within the spike trains of individual RGCs are necessary to recover the behavioral discrimination performances. Along the same line of thought, it was shown in [24] that 90% of the information about the stimuli can be retrieved from the firing activity of RGCs considered as independent encoders.

However, there is a growing body of evidence that considering RGCs as synergistic encoders carries complementary and more precise information about the stimulus. By synergistic, we mean that the concerted spiking pattern in a population of RGCs will carry more information about the stimulus than the sum of the information contained in the spiking of individual RGCs assumed as independent. The functionnal significance of the concerted firing pattern has been investigated using a model of multi-neuron spike responses [27]. The authors showed that model-based decoding that exploits the response correlation structure extracts 20% more information about the stimulus than decoding under the assumption of independence, and preserves 40% more visual information than optimal linear decoding and thus, correlations provide additional sensory information about the stimulus. In [32], when flashing 36 black and white shapes onto salamander retinas, the authors reported that simple linear decoders, i.e., decoders based on independent spike train coding strategies, can only decode for coarse stimulus properties such as the overall size or contrast. To perform high-fidelity discrimination, one needs non-linear decoders that take into account correlations between RGC responses. Another interesting result was obtained by [11] when flashing gratings of varying phase. The authors showed that the differential spike latencies (i.e., the relative timing between the latency of some pairs of RGC) is tuned to the phase of the grating and thus can encode spatial information. These results were obtained by focusing on the fast-OFF cells that exhibit a low level of spontaneous activity and respond to both increases and decreases in light intensity in the receptive field [11,39]. Based on their results, the authors suggested that "*a population code based on differential spike latencies could be a powerful mechanism to rapidly transmit new visual scenes*".

In this study we have tested whether differential spike latencies are an equally powerful mechanism for encoding information about the stimulus in the mammalian retina. To adress this question we have used sets of flashed gratings of differing spatial frequencies and phases. We recorded the light-induced spiking activity from 469 RGCs from 5 mouse retinas using a 60-channel multielectrode array (see Methods). Three main results are discussed. First we show that differential spike latencies, in our experiments, are not sufficient to discriminate between stimuli considering only single RGC pairs, so we decided to extend the analysis to all possible

RGC pairs. Taking into account all the possible pairs describes a spatio-temporal spike pattern that is at the core of the analysis: how does the shape of the wave of first spikes (WFS) recorded from all responsive RGCs vary with the stimuli? To read out this WFS several algorithms can be used [30]. Here we chose to focus on the rank order code (ROC), which classifies each neuron on the basis of the relative rank of the first stimulus-evoked spikes. In particular, it should be noted that this method is based on ranks, thus ignoring the precise absolute timing of individual spikes. The motivation for using this method is to make a direct link with previous work on ROC as a coding strategy [35], established in the context of ultra-fast visual categorization where the human visual system can analyze and classify a new complex scene in less than 0.150 sec [36, 20, 9]. It has been shown that ROC has computational advantages such as fast processing and robustness compared to classical rate- and latency-based independent coding strategies [38]. However, to our knowledge, the relevance of the WFS for a whole RGC population read-out by a ROC has never been shown at the level of the retina. Then we investigate the power of the WFS using a discrimination task. At a given grating spatial frequency, the task is to indentify the correct phase from a set of RGC responses to a given grating. We measured the discrimination performances as a function of the spatial frequency and then we compared the performances of the ROC decoder versus classical rate- and latency-based independent decoders using a Bayesian classifier. We also investigate the impact of a simple neuronal layer on the WFS, simulating the fact that RGC responses are transmitted via the optic nerve to retinal targets such as the lateral geniculate nucleus (LGN). We fed a simulated LGN-like layer [23] (see Methods) with the experimental spikes and then analyzed the LGN-like output spikes using the same discrimination task as before. Finally, we compare the discrimination performances of the rate, the latency, and the ROC decoders by varying the length of the observation window after the stimulus onset in order to highlight the capabilities of fast transmission of the visual information.

2 Methods

2.1 Retinal recordings

All experimental procedures were approved by the UK Home Office, Animals (Scientific procedures) Act 1986. We used C57BL/6 mice aged 19-46 days postnatal. The animals were dark-adapted overnight prior to retinal isolation. On the day of the experiment, the mouse was sacrificed by cervical dislocation, both eyes were quickly enucleated and placed in artificial cerebrospinal fluid (aCSF) containing,the following (in mM): 118 NaCl, 25 NaHCO3, 1 NaH2 PO4, 3 KCl, 1 MgCl2, 2 CaCl2, and 10 glucose, equilibrated with 95% O2 and 5% CO2. The retina was isolated from the eye cup and flattened, RGC layer facing down, onto the bottom of a 60-channels ITO MEA (60MEA200/30iR-ITO; MultiChannel Systems, Reutlingen, Germany). Throughout recording, retinas were maintained at 32°C and perfused with aCSF at a rate of 1ml/min. All surgical procedures were performed under dim red light and the room was maintained in darkness throughout the experiment. Extracellular signals were acquired using an MEA1060-Inv amplifier, digitized and sampled at 25 kHz by an MC_Card data acquisition card and recorded using MC_Rack (MultiChannel Systems). Action potentials were extracted offline in MC_Rack using a voltage threshold set at 6.5-8 standard deviations below the signal recorded on each channel during a baseline recording taken at the start of each experiment, before the retina was placed on the MEA. Spike sorting was done automatically using the T-Distribution Expectation-Maximisation algorithm in Offline Sorter (Plexon Inc, Dallas, USA). Sorted units were then verified manually; any units with greater than 1% of inter-spike intervals less than 0.001 sec or without a clear, action potential-like waveform were rejected.

2.2 Stimulus design

The stimuli used in this study were square wave gratings with varying spatial frequency and phase. We used 4 different bar widths: 1600µm, 800µm, 400µm, and 200µm. As 1°= 30 µm onto the mouse retina [29] the 4 bar widths correspond to spatial frequencies of 0.008, 0.016, 0.034, and 0.069 cpd. For each spatial frequency, we define 8 phases by shifting the gratings by $\frac{1}{4}\times$the bar width. The stimuli were flashed for 0.5 sec followed by a uniform gray mask flashed for 1 sec. Each stimulus was presented 150 times in randomized blocks of 32 stimuli (4 bar widths $\times$ 8 phases). We presented the stimuli using a 6.5" LCD monitor (640x480px, 60Hz refresh rate), focused onto the RGC layer using a pair of lenses (Edumund Optics, Barrington, USA) and a 2X objective on an Olympus IX-71 inverted microscope (Olympus, Tokyo, Japan). Stimuli were generated in Matlab (MathWorks, Natick, USA) and controlled using Psychtoolbox [4, 26, 21].

2.3 Kendall *tau* distance

Considering the RGCs population responses as rankings based on the latencies of spikes, as a first analysis, we estimate the differences between two rankings related to two different stimulus. To measure the difference between those rankings we used the Kendall *tau* rank distance denoted by τ [19]. This metric counts the number of pairwise disagreements between two rankings. If n is the number of RGCs, D the number of pairs that are discordant between the two rankings, then the Kendall *tau* distance is :

$$\tau = \frac{D}{n(n-1)/2}$$

The τ-distance varies from 0 if the two rankings are similar, to 1 if the rankings are in the opposite order; in other words, the larger the distance, the more dissimilar the two lists are.

2.4 Decoding RGC spike trains: the discrimination task

As mentioned in the text, we used a discrimination task to quantitatively evaluate the power of the WFS in encoding stimulus information. In the task, at given a spatial frequency, the grating is presented at 8 different phase. Each stimulus is presented 150 times producing a corresponding set of responses. Given 75 trials randomly chosen as training set for each stimulus $\varphi \in \{1..8\}$ and the responses from the remaining 75 trials of a tested stimulus $\bar{\varphi}$, we sought to determine which grating phase the response corresponds to.

To solve this question, a classical Bayesian classifier was used, thus allowing different codes to be tested within the same formalism. For each phase $\bar{\varphi}$, we estimated the phase $\tilde{\varphi}$ using the maximum likelihood criterion

$$\tilde{\varphi} = \underset{\varphi\in\{1..8\}}{\operatorname{argmin}}\{-\log(P(\varphi|r_{\bar{\varphi}}))\},$$

where $r_{\bar{\varphi}}$ represents the set of responses from the tested phase. Classically, we used the Bayes Theorem to estimate $P(\varphi|r)$ from the response distribution $P(r|\varphi)$ which depends on the code chosen. To test the rate code, r is the average number of spikes within the presentation time of the stimulus, when each neuron is considered as independent. Similarly, to test the latency code, r is the latency of the first spike after the stimulus onset. Finally, to test the ROC code based on the WFS, r is the rank of latency time after stimulus onset for each neuron, which can be directly obtained from estimating the relative ordering between all pairs of RGCs. In that case, for a RGC pair (i, j), the response distribution is defined by

$$P(r_{(i,j)}|\varphi) = C\sum_{T} H(L_i^T - L_j^T),$$

where L_i^T is the latency of neuron i for trial T in the training set, C is a normalisation factor and

$$H(s) = \begin{cases} 0 & \text{if } s \leq 0, \\ 1 & \text{otherwise.} \end{cases}$$

For each stimulus $\bar{\varphi}$ tested, 150 different configurations of training set and test set were randomly chosen. Each time the Bayesian classifier was applied to guess the phase $\tilde{\phi}$. Results were stored in a 8×8-confusion matrix M ($M(\tilde{\varphi}, \bar{\varphi})$ was incremented after every classification). Each column of M represents the results over all configurations when a given phase $\bar{\varphi}$ was tested. If the maximum lies along the diagonal, then the image has beencorrectly decoded in a plurality of configurations. To quantify the performance, we estimated the fraction of correct predictions as the mean of the diagonal of the confusion matrix. The fraction of correct predictions is in $[0, 1]$. If $\tilde{\varphi}$ is equal to $\bar{\varphi}$ for all $\bar{\varphi}$ tested and all trials, the fraction of correct prediction will be 1. Using this approach, the fraction of correct predictions is shown in Figures 3A and 1C for the different codes and as a function of the frequency of the gratings. To compute the evolution of the performance with the number of RGCs shown in Figure 3B and 1D, the fraction of correct predictions is estimated and averaged over 100 randomly chosen RGC subsets ranging from 2 RGCs to the whole available RGC population.

2.5 Artificial LGN layer

To investigate the impact on the neural code of a later processing stage, the recorded spikes were fed into a LGN-like layer as defined in [23]. Briefly, the relay cells were modelled with the Spike Response Model (SRM) [10]. The artificial LGN was restricted to monosynaptically connected LGN cells, organized in one retinotopic layer of 469 neurons. Then, the spikes from the LGN output were analyzed using the same discrimination task.

3 Results

3.1 Most RGC pairs do not discriminate between stimuli

We begin by considering single pairs of RGCs to verify whether differential spike latencies could discriminate between different stimuli. In 469 RGCs recorded from five retinas we did not find any RGC pairs that exhibited a clear stimulus-driven correlation for all phases. Figure 1A–B shows the typical behavior we observed for latencies (L_1, L_2) of a RGC pair, as a function of the stimulus: there is no tuning of the absolute latencies with the phase of the grating. In support of this finding, we estimated the percentage of RGC pairs allowing the discrimination of a given number of stimuli pairs. To this aim, for each pair of neurons (n_i, n_j), we estimated the number of pairs of stimuli which could be significantly discriminated by looking at the distributions of latencies (L_i, L_j). We used a 2D-Kolmogorov-Smirnov test [25] to determine wether there were significant differences. Results are shown in Figure 1E: 93.2% of the RGC pairs cannot discriminate any stimulus pair and only two RGC pairs were able to discriminate between 25 stimulus pairs. However, even for these two RGC pairs the distributions of their latencies (L_1, L_2) are still not clearly distinguishable (insets in Figure 1E). This may be due to the presence of strong baseline spontaneous activity which introduces considerable variability in latency values, as can be seen in Figure 1D. However, despite the fact that the absolute value of latencies in individual RGCs is noisy, it may be that the relative timing between RGCs is reliably preserved. However, Figure 1C shows that there is no tuning of the relative timing $(L_1 - L_2)$ between cells in pairs.

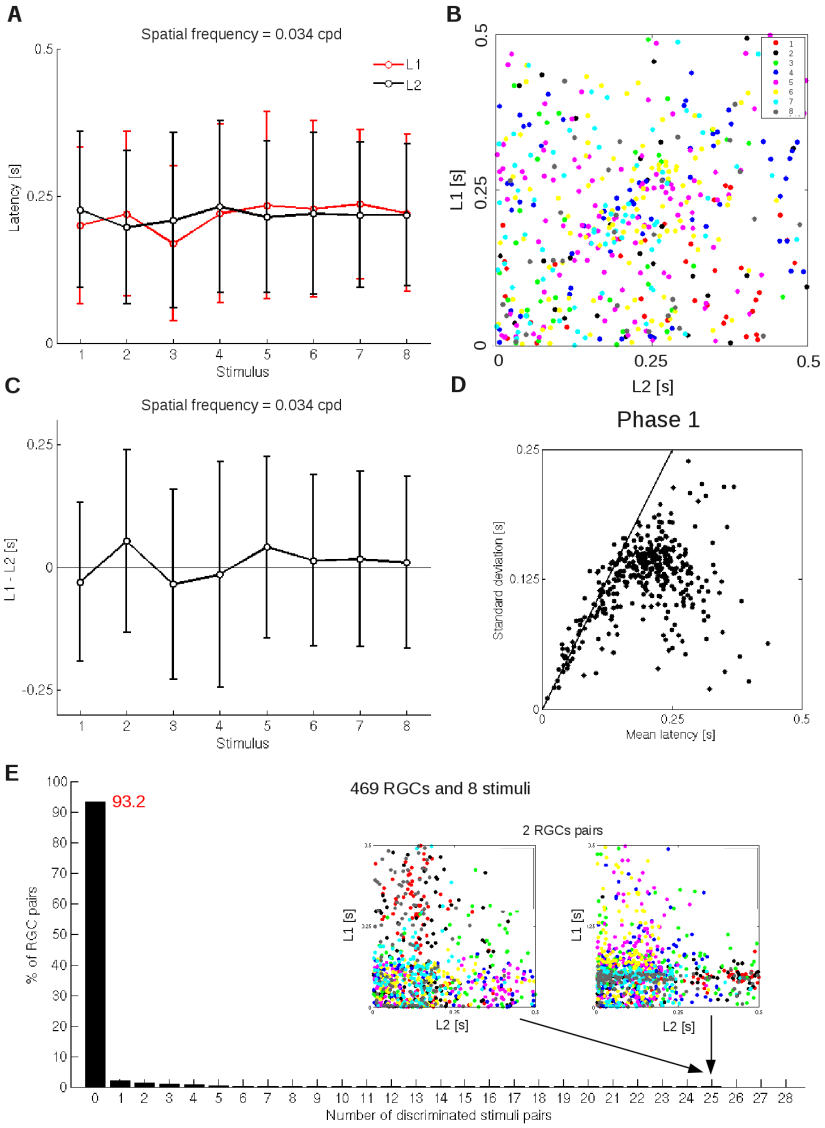

Figure 1: **Latencies of a RGC pair for gratings of spatial frequency of 0.034 cpd (8 phases).** (A) Latencies L1 and L2 of a tipical RGC pair, averaged over the trials as a function of the grating phase. (B) Scatter-plot of latencies (L_1, L_2) for the same RGC pair. Each color stands for one phase of the grating. (C) Latency difference $L_1 - L_2$ averaged across trials. (D) Concidering the phase $\varphi = 1$, the standard deviation is plotted as a function of the mean latency over the trials, for all the 469 recorded RGCs. The black line corresponds to $y = x$. (E) Percentage of RGC pairs as a function of the number of discriminated stimuli pairs. Stimuli are the 8 gratings differing with the phase, giving 28 pairs of stimuli. Results show that 93.2% of RGC pairs do not allow to discriminate any pair of stimuli and that no RGC pair can discriminate more than 25 stimuli pairs. In the best case, two neurons pairs are found for 25 image pairs: Insets show their relative latency distributions. The error bars in (A) and (C) represent the standard deviation.

These observations differ from the results shown in [11] in salamander with fast-OFF RGC pairs, where the latencies of some RGCs were tuned to the phase of the gratings and thus one RGC pair could clearly discriminate between the eight stimuli (see, e.g., the Figure 2B from [11]). These differences can also be quantified at the population level. In [11], the authors reported a correlation coefficient of the latencies averaged over all stimuli and RGC pairs equal to 0.25±0.04. By doing the same computation on our recordings, we observed an averaged correlation coefficient of latencies equal to 0.002±0.021.

3.2 The WFS provides spatial cues about the stimulus

Since we found that in mice single RGC pairs are not capable of discriminating between different stimuli, we extendeds the analysis to the whole set of RGC pairs, i.e. the WFS. To quantify the difference between the WFS obtained under different stimulation conditions, we used the Kendall tau rank distance (τ) [19]. This metric counts the number of pairwise disagreements between two rankings (see *Methods*). The larger the distance, the more dissimilar the two lists are. The τ-distance varies from 0 (if the two rankings are similar) to 1 (if the rankings are in the opposite order). Figure 2A shows the τ-distance between gratings of phases 1 to 8. The τ-distance is computed using the binarized average-rankings across all trials. For example, the distance between the gratings of phase 1 and 5 is $\tau(1,5) = 0.0676$: This means that for 6.76% of the 109746 possible RGC pairs (number of pairs $= (n(n-1))/2$, with $n = 469$), that is 7418 RGC pairs, their relative ranks have changed between the phases 1 and 5. Given grating 1 as a reference, one can plot the variations of $\tau(1,\varphi)|_{\{\varphi=2..8\}}$ where φ are the phases of the other gratings. Results are shown in Figure 2B (solid black line): $\tau(1,\varphi)$ is low for nearby phases and high for phases $\varphi = 4$ to 6. The τ-distance varies cyclically with the phase of the gratings demonstrating that the WFS should encode for spatial cues about the stimulus.

In order to have a first overview of the encoding capabilities of the WFS, one can focus on the subset of neurons with the shortest latencies. To do so we consider the subset of 211 RGCs that respond on average within 0.15 sec after the onset of the gratings of 0.034 cpd spatial frequency. Using these neurons, the τ-distance is again estimated and $\tau(1,\varphi)|_{\{\varphi=2..8\}}$ is shown in Figure 2B (grey dashed line). Results show that in average 89% of τ-distance obtained with the whole RGC population can be retrieved considering only roughly half of the RGC population. Already within 0.15 sec after the onset of the gratings, the WFS can capture 89% of the differences between the stimuli observed at 0.5 sec.

3.3 The WFS provides efficient coding capability

To quantify the coding capability of the WFS, the discrimination task was to identify which of the eight gratings is presented for a fixed spatial frequency (see Methods). The results are shown in Figure 3A and B where we compare the fraction of correct identifications for the rate code (green), the latency code (red), and the ROC (blue).

Firstly, we show that the WFS is able to discriminate between stimuli. Figure 3A shows the fraction of correct identifications as a function of the spatial frequency of the gratings. In this analysis, we considered all 469 experimental RGCs and all spikes occurring within the first 0.5 sec following stimulus onset. All the tested decoders performed better than chance (chance level $= 1/8 = 0.125$) at all spatial frequencies. The fraction of correct identifications for both the rate and the ROC is greater than 0.75 for the three lowest spatial frequencies. The performance of the ROC is close to the performance of the rate code and better than the latency code, suggesting that the WFS is more robust to the noise coming from the spontaneous activity than the absolute spike latencies. Another observation is that performance of the latency code is

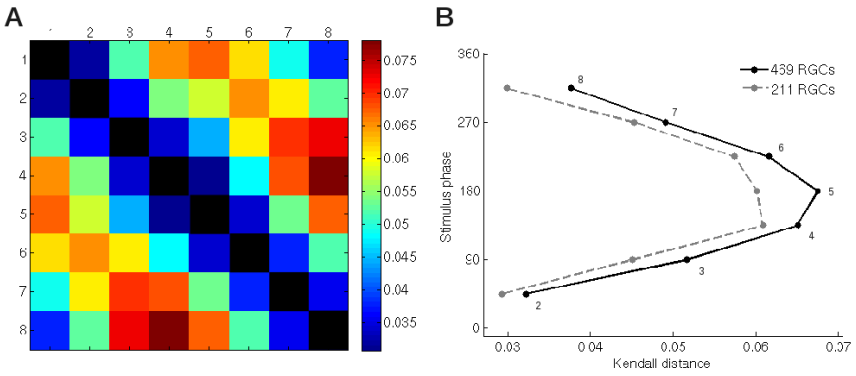

Figure 2: **The wave of first spikes (WFS) is characteristic of the stimulus.** Here is concidered the gratings of spatial frequency equal to 0.034 cpd. (A) Matrix showing the Kendall *tau* distance (τ) computed for all possible stimuli pairs: $\tau = 0$ for strictly identical ranked lists and $\tau = 1$ for ranked list that are strictly opposite. (B) Plot of the first line of the matrix represented in (A) showing the variations of $\tau(1, \varphi)|_{\{\varphi=2..8\}}$ where φ are the other gratings differing with their phases.

considerably impaired at the lowest spatial frequency, i.e., the largest bar width.

Secondly, we show how the decoders performance varies with the size of the RGC population. Figure 3B shows the evolution of the fraction of correct identifications as a function of the number of RGCs. For all the decoders, the performance increases with the number of neurons. The rate decoder gives the best discrimination performance (considering only gratings of spatial frequency 0.034 cpd where the rate code outperformed the other codes for the entire population). This difference in code performance is independent of the number of neurons. The ROC performs better than the latency decoder even with few neurons.

3.4 The WFS and higher neural structures

Since the retinal response is conveyed to and processed in retinal projection areas, such as the LGN, we investigated the possible effects of a post-processing neural layer on the neural code. We fed the spikes obtained from our recordings into an artificial LGN-like layer [23]. It appears that the main effect of this LGN layer is to filter out some spontaneous activity which is in agreement with experimental results [28], where spikes that are isolated in time are not relayed (at least two RGC input spikes with a short inter-spike interval (0.15-0.20 sec) are needed to elicit a LGN spike). We then analyzed the output spikes of the 388 active LGN neurons using the same discrimination task and the same Bayesian classifier as before.

The fraction of correct identifications for the different methods is shown in Figure 3C (compare with Figure 3A). Differences between the decoders are enhanced: the overall performance of the rate and latency decoders decreases and both are clearly outperformed by the ROC decoder.

The effect of the size of the population, is shown in Figure 3D (compare with Figure 3B). Three interesting observations can be made. The ROC decoder rapidly outperforms the other decoders with only 50 LGN neurons or more; The maximum ROC performance obtained with RGC neurons is reached with fewer LGN neurons (0.75 with less than 250 LGN neurons). The maximum ROC performance obtained with LGN neurons is 0.90 (388 neurons). Therefore, the WFS is not only preserved, but even refined through the LGN-like layer.

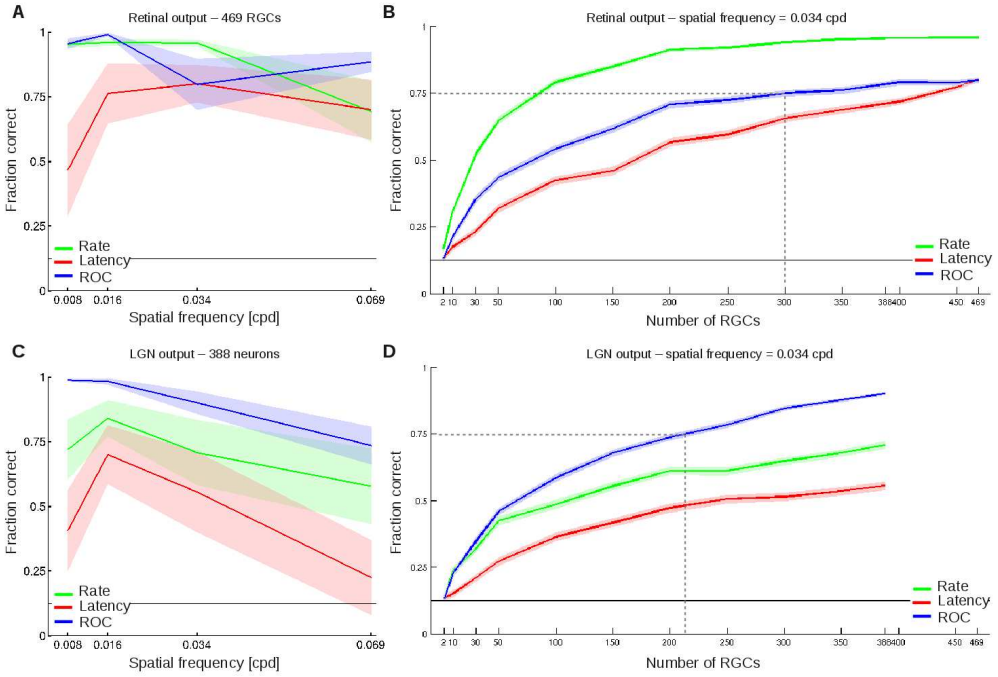

Figure 3: **Discrimination performance of the rate, latency, and ROC decoders.** The fraction of correct identifications is plotted for the rate code (green), the latency code (red), and the ROC (blue). In (A) and (B) the responses of the retinal output are considered (469 RGCs). (A) Fraction of identifications as a function of the spatial frequency. (B) Fraction of correct identifications concidering the gratings of spatial frequency equal to 0.034 cpd as a function of the number of neurons. In (C) and (D) the responses of the simulated LGN output are concidered (388 neurons). (C) Fraction of correct identifications as a function of the spatial frequency. (D) Fraction of correct predictions concidering the gratings of spatial frequency equal to 0.034 cpd as a function of the number of neurons. In all plots, the shaded areas represent the standard error of the mean. The chance level of the discrimination task ($1/8 = 0.125$) is represented by a black line

3.5 The WFS enables fast transmission of visual information

We investigated the fast transmission capabilities by computing the fraction of correct identifications as a function of the time window: an observation window ranging from 0.05 sec to 0.5 sec after the stimulus onset. Given the responses related to the gratings of spatial frequency 0.034 cpd, we compared the performances of the rate, the latency, and the ROC decoders (Figure 4). Figure 4A shows the results using the recorded RGCs. Overall, the performances of all decoders increase as the length of the observation window increase. The rate decoder performances increase the fastest and reach its maximum with a 0.35 sec observation window. The interesting point is the ROC decoder follows closely the rate decoder and outperforms the latency decoder during the firsts hundreds of milliseconds after the stimulus onset. With an observation window of 0.15 sec, the rate and the ROC decoder share the same discriminations performance respectively 0.45 ± 0.17 and 0.45 ± 0.12, while the latency decoder is close to the chance level (0.15 ± 0.12). Figure 4B shows the results using the simulated-LGN responses. Also here the dif-

ferencies between the decoders are enhanced. The performances of the rate and latency decoders are both clearly outperformed by the ROC decoder with a 0.15 sec observation window and more. With an observation window of 0.15 sec, while the rate and the latency decoder performances are impaired, with respectivelly 0.18 ± 0.12 and 0.31 ± 0.14, the ROC decoder already allow to discriminate between the stimuli with a fraction of correct indentiofations equals to 0.51 ± 0.08.

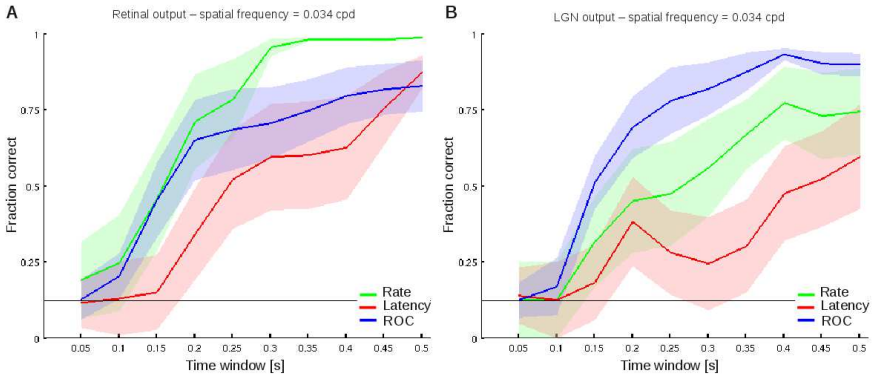

Figure 4: **Discrimination performance as a function of the time window after the stimulus onset.** The fraction of correct identifications is plotted for the rate code (green), the latency code (red), and the ROC (blue), as a function of the considered time window after the stimulus onset. Only responses related to the gratings of spatial frequency equal to 0.034 cpd are used in this analysis. (A) The responses of the retinal output are considered (469 RGCs). (B) The responses of the simulated LGN output are concidered (388 neurons). In all plots, the shaded areas represent the standard error of the mean. The chance level of the discrimination task ($1/8 = 0.125$) is represented by a black line.

4 Discussion

4.1 Latency correlation between pairs of RGCs in mouse

In this study on the mouse retina, we did not find any RGC pairs exhibiting a clear correlation between their latencies in responses to a set of gratings of varying phase (Figures 1A and 1C). We also observed an averaged coefficient correlation of latencies equal to 0.002 ± 0.021, which is clearly lower than the one observed in salamander (0.25 ± 0.04, see supplemental data in [11]). Our results on the latency correlations between RGC pairs also lead to different conclusions than in [11] where the authors were focusing on fast-OFF RGCs. In our experiments, single RGC pairs are not sufficient to encode spatial cues about the stimulus and this may be due to two factors. Firstly, spontaneous firing may have masked the possible latency correlations between RGC pairs. Secondly in [11], it is important to emphasize that only two to eight fast-OFF RGCs per retina were found to share strong correlations for any given experimental retina (nine retinas were used in total, supplemental data in [14]). Therefore, one could ponder whether these low numbers reflect real biological scarcity of these specific neurons within the overall RGC population, or alternatively, whether only few pairs were detected because a 60 or 252-channels MEA can record only from a fraction of the entire RGC population. To answer this question, one could conduct further experiments using new high density MEAs such as [3, 22, 2] allowing

the simultaneous recording from thousands of RGCs.

4.2 Limits of the latency coding with respect to the spatial frequency

Our study reveals some complementary results with respect to [17] where gratings of varying frequency were also used in mouse to compare the performance of a behavorial task with electrophysiological recordings. They used a two-alternative forced choice visual discrimination task with sinusoidal gratings of spatial frequency ranging from 0.035-0.5 cpd, corresponding approximately to 428-30μm onto the mouse retina. They observed that performance dropped to chance level when the spatial frequency was high, i.e., at 0.5 cpd, which is consistent with the maximum measured acuity at the retinal level [31] or LGN level [13]. In this paper, we chose a different range of frequencies, from 0.009-0.075 cpd, which should be perfectly perceived at the retinal level. For our highest frequencies, result are comparable with [17]. However, note that the highest spatial frequency used here does not allow investigating the limits of retinal visual acuity (as in [17]), where the drop is observed. On the other hand, we tested what happens with a lower spatial frequency, and we found that the performance of the latency decoder for the 0.009 cpd frequency is lower than the performance for the 0.018 cpd frequency (Figure 3A). We suggest that the edges of the gratings fall within the receptive field of fewer RGC as the spatial frequency decreases. Thus, at the entire RGC population level, only a few cells would encode the different phases of the gratings.

4.3 Relevance of the WFS and decoding strategies

Despite the high variability of the absolute latencies, one could hypothesize that the time of occurrence of the first spikes following the stimulus tend to vary in concert within the whole RGC population on each trial, resulting in the preservation of the spike timing between RGC according to the stimulus. We found that considering single RGC pairs does not support this hypothesis (see example in Figure 1C). Then we investigated this hypothesis at the population level, by computing the ranks of the first stimulus-driven spikes for the entire population of RGCs, i.e., the WFS. The distance between two retinal responses associated with two different stimuli was evaluated using the Kendall τ-distance which measures the number of pairwise disagreements between two ranking lists (Figure 2C and 1D). We found a strong dependence of the Kendall τ-distance on the phase of the stimulus. This means that a specific stimulus triggers responses in a population of RGCs with a specific timing signature based on spike ranking.

To decode the WFS, several strategies can be used. Assuming that the firing order is stimulus-specific, the simplest algorithm is the winner-take-all decoder [1]. In this decoder, for an incoming firing pattern across the entire RGC population, the decision of the classifier is determined by the RGC with the shortest latency. But this decoder can be unreliable, especially if the timing of incoming spikes is not reliable, e.g. due to spontaneous activity (as observed in our recordings), or if spikes generated by different cells occur in very short succession, or become completely synchronous. Another possibility is to consider the spatiotemporal patterns of all spikes in a spike train within a given time window and use the tempotron algorithm [15]. The tempotron consists of a single integrate-and-fire model neuron (IF) that receives inputs from the population of RGCs. Depending on the relative timing of the incoming spikes and their synaptic weights (that are *a priori* determined; supervised algorithm), the summation of all the inputs will determine whether the IF neuron will fire or not. Thus, this model can classify the input spikes patterns into those that elicit a spike in the IF neuron, and those that do not trigger the IF neuron. The tempotron was used to analyze salamander retinal responses and was able to decode complex visual features [14]. The authors applied this decoding strategy to fast-OFF RGCs, using a total

of only 41 cells recorded from nine retinas. However, how this coding scheme would behave with other RGC subtype or with a mixture of RGC subtypes, and how performance will be affected using a larger RGC population, are opened questions.

In this study we have applied a simpler (unsupervised) decoding strategy based on the ROC decoder [35] onto the whole RGC population (469 RGCs in 5 retinas), regardless of their specific functional subtypes. Here the spatio-temporal spike pattern is represented by the rank of spikes within the WFS. To assess the performance of the ROC decoder, we designed a discrimination task where the goal was to identify the phase of the gratings. We found that the ROC decoder performs much better than the decoder using independent RGC latencies (Figure 3A), and in addition, performance was higher even with few cells (Figure 3B). Regardless of the RGC subtype and the level of spontaneous activity, the main conclusion is that the WFS already contains sufficient spatial cues about the stimuli to succeed in this discrimination task.

An interesting perspective would be to further investigate the specific role of each sub-populations of RGCs within the WFS. A first step could be to focus as in [11] on fast-OFF RGCs since an analogous subtype has been reported in the mouse retina [6]. More generally, one could consider an ensemble of discrimination tasks and determine which sub-populations, based on RGC morphological and functional properties, are relevant for each task since there is evidence that different RGC subtypes encode different features of the stimuli [40,37].

4.4 The WFS is transmitted to higher neural structures

We investigated the possible effects on the discrimination performance of a later processing stage. To do so, we fed a simulated LGN-like layer as defined in [23] with the RGC spikes. We then analyzed the simulated LGN spikes using the same methods. We showed that the ROC decoder performs even better when using the spikes from the LGN layer than from RGC. Using the WFS from the LGN layer, not only we reached the peak performance obtained using RGC responses with fewer neurons, but we clearly outperformed the classical rate and latency decoders with the whole population of RGCs. This simple post-processing stage interpreted at the LGN layer enhances the discrimination performance of our ROC decoder, while the classical rate and latency decoders become impaired. The reason is that this LGN layer filters out some of the spontaneous activity. Spikes that are isolated in time are not relayed and as a consequence this LGN layer refines the reliability of the spike timing and condenses the information about the visual scene. These observations are in line with recent findings demonstrating that spikes relayed by the LGN in cats are more reliable in their timing [28]. LGN processing increases sparseness in the neural code by selectively relaying the highest fidelity spikes to the visual cortex. Thus, the LGN shapes the visual signal before it reaches the cortex [28] and the information from the WFS becomes even more relevant.

4.5 The WFS conveys visual information faster than classical coding scheme

We finally investigated the capabilities of fast transmission of the visual information by comparing the discrimination performances of the rate, the latency and the ROC decoders as a function of the time window after the stimulus onset (Figure 4A-4B). Already at the level of the retinal output, the results show that a decoder that exploits the WFS, here the ROC decoder, allows to reach a level of performances 0.1 sec faster than a classical latency decoder (Figure 4A). This observation is even enhanced when using the responses from the LGN layer, where the ROC decoder performances increase faster and sooner than the rate and the latency decoder performances ((Figure 4B). These results are in line with previous studies [35,16,38] which have

suggested that the WFS could be an efficient and fast encoding process of the visual information. Here we show that this is indeed the case for a whole RGC population. And to our knowledge, reading-out this WFS with a ROC has never been shown at the level of the retina.

4.6 The WFS in other sensory systems

In this study we have shown that the WFS encodes meaningful information about the stimulus at the level of the retina. How neurons fire with respect to each other is of fundamental importance for understanding neural codes in other sensory systems as well. In the olfactory system, the WFS and spike-timing in neuronal ensembles play an important role in information encoding [33, 34]. In the tactile sensory system, it has been shown that the relative timing of the first spikes after the stimulation onset contains rich information about the stimulus, such as the direction, the force, and the shape of the surface contacting the fingertip [18]. Similar observations have also been reported in the auditory system [8, 7, 5]. All these results reveal the generality and power of the WFS which represents a common denominator in various sensory modalities. The WFS conveys enough information for the encoding and fast transmission of relevant sensory information to the brain, allowing it to process and produce fast appropriate responses.

5 Acknowledgments

The research received financial support from the 7th Framework Programme for Research of the European Commission (Grant agreement no 600847: RENVISION project of the Future and Emerging Technologies (FET) programme (Neuro-bio-inspired systems (NBIS) FET-Proactive Initiative)) (PK, ES) and the Wellcome Trust (grant number 096975/Z/11/Z) (JMB, ES). The authors would like to thank Bruno Cessac, Matthias Hennig and Gerrit Hilgen for their insightful that helped to improve the manuscript.

References

[1] JA Barnden and K Srinivas. Temporal winner-take-all networks: A time-based mechanism for fast selection in neural networks. *Neural Networks, IEEE Transactions on*, 4(5):844–853, 1993.

[2] L Berdondini, A Bosca, T Nieus, and A Maccione. *Nanotechnology and Neuroscience: Nano-electronic, Photonic and Mechanical Neuronal Interfacing*, chapter Active Pixel Sensor Multielectrode Array for High Spatiotemporal Resolution, pages 207–238. Springer, 2014.

[3] Luca Berdondini, Kilian Imfeld, Alessandro Maccione, Mariateresa Tedesco, Simon Neukom, Milena Koudelka-Hep, and Sergio Martinoia. Active pixel sensor array for high spatio-temporal resolution electrophysiological recordings from single cell to large scale neuronal networks. *Lab on a Chip*, 9(18):2644–2651, 2009.

[4] D.H. Brainard. The Psychophysics Toolbox. *Spatial Vision*, 10:433–436, 1997.

[5] Romain Brasselet, Stefano Panzeri, Nikos K Logothetis, and Christoph Kayser. Neurons with stereotyped and rapid responses provide a reference frame for relative temporal coding in primate auditory cortex. *The Journal of Neuroscience*, 32(9):2998–3008, 2012.

[6] Stephen M Carcieri, Adam L Jacobs, and Sheila Nirenberg. Classification of retinal ganglion cells: A statistical approach. *J Neurophysiol*, 90:1704–1713, 2003.

[7] Steven M Chase and Eric D Young. First-spike latency information in single neurons increases when referenced to population onset. *Proceedings of the National Academy of Sciences*, 104(12):5175–5180, 2007.

[8] R Christopher deCharms and Michael M Merzenich. Primary cortical representation of sounds by the coordination of action-potential timing. *Nature*, 381:13, 1996.

[9] Sébastien M Crouzet, Holle Kirchner, and Simon J Thorpe. Fast saccades toward faces: face detection in just 100 ms. *Journal of Vision*, 10(4):16, 2010.

[10] Wulfram Gerstner, Raphael Ritz, and J Leo Van Hemmen. Why spikes? hebbian learning and retrieval of time-resolved excitation patterns. *Biological cybernetics*, 69(5-6):503–515, 1993.

[11] T. Gollisch and M. Meister. Rapid neural coding in the retina with relative spike latencies. *Science*, 319:1108–1111, 2008. DOI: 10.1126/science.1149639.

[12] M. Greschner, A. Thiel, J. Kretzberg, and J. Ammermüller. Complex spike-event pattern of transient on-off retinal ganglion cells. *J Neurophysiol*, 96:2845–2856, 2006.

[13] Matthew S Grubb and Ian D Thompson. Quantitative characterization of visual response properties in the mouse dorsal lateral geniculate nucleus. *Journal of neurophysiology*, 90(6):3594–3607, 2003.

[14] Robert Gütig, Tim Gollisch, Haim Sompolinsky, and Markus Meister. Computing complex visual features with retinal spike times. *PLoS ONE*, 8(1):e53063, January 2013.

[15] Robert Gütig and Haim Sompolinsky. The tempotron: a neuron that learns spike timing–based decisions. *Nature neuroscience*, 9(3):420–428, 2006.

[16] R. Guyonneau, R. vanRullen, and S.J. Thorpe. Neurons tune to the earliest spikes through stdp. *Neural Computation*, 2004. In review.

[17] A.L. Jacobs, G. Fridman, R.M. Douglas, N.M. Alam, P.E. Latham, G.T. Prusky, and S. Nirenberg. Ruling out and ruling in neural codes. *Proceedings of the National Academy of Sciences*, 106(14):5936–5941, 2009.

[18] Roland S Johansson and Ingvars Birznieks. First spikes in ensembles of human tactile afferents code complex spatial fingertip events. *Nature neuroscience*, 7(2):170–177, 2004.

[19] M. G. Kendall. A new measure of rank correlation. *Biometrika*, 30(1-2):81–93, 1938.

[20] Holle Kirchner and Simon J. Thorpe. Ultra-rapid object detection with saccadic eye movements: Visual processing speed revisited. *Vision Research*, 46(11):1762 – 1776, 2006.

[21] M. Kleiner, D.H. Brainard, and D.G. Pelli. What's new in Psychtoolbox-3? *Perception*, 36:ECVP Abstract Supplement, 2007.

[22] Alessandro Maccione, Matthias H Hennig, Mauro Gandolfo, Oliver Muthmann, James Coppenhagen, Stephen J Eglen, Luca Berdondini, and Evelyne Sernagor. Following the ontogeny of retinal waves: pan-retinal recordings of population dynamics in the neonatal mouse. *The Journal of physiology*, 592(7):1545–1563, 2014.

[23] T. Masquelier. Relative spike time coding and stdp-based orientation selectivity in the early visual system in natural continuous and saccadic vision: a computational model. *Journal of Computational Neuroscience*, 32(3):425–441, 2012.

[24] Sheila Nirenberg, SM Carcieri, AL Jacobs, and Peter E Latham. Retinal ganglion cells act largely as independent encoders. *Nature*, 411(6838):698–701, 2001.

[25] JA Peacock. Two-dimensional goodness-of-fit testing in astronomy. *Monthly Notices of the Royal Astronomical Society*, 202:615–627, 1983.

[26] D.G. Pelli. The VideoToolbox software for visual psychophysics: Transforming numbers into movies. *Spatial Vision*, 10:437–442, 1997.

[27] Jonathan W Pillow, Jonathon Shlens, Liam Paninski, Alexander Sher, Alan M Litke, EJ Chichilnisky, and Eero P Simoncelli. Spatio-temporal correlations and visual signalling in a complete neuronal population. *Nature*, 454(7207):995–999, 2008.

[28] Daniel L Rathbun, David K Warland, and W Martin Usrey. Spike timing and information transmission at retinogeniculate synapses. *The journal of neuroscience*, 30(41):13558–13566, 2010.

[29] S Remtulla and PE Hallett. A schematic eye for the mouse, and comparisons with the rat. *Vision research*, 25(1):21–31, 1985.

[30] F. Rieke, D. Warland, R. de Ruyter van Steveninck, and W. Bialek. *Spikes: Exploring the Neural Code*. Bradford Books, 1997.

[31] Francesco Mattia Rossi, Tommaso Pizzorusso, Vittorio Porciatti, Lisa M Marubio, Lamberto Maffei, and Jean-Pierre Changeux. Requirement of the nicotinic acetylcholine receptor $\beta 2$ subunit for the anatomical and functional development of the visual system. *Proceedings of the National Academy of Sciences*, 98(11):6453–6458, 2001.

[32] G. Schwartz, J. Macke, D. Amodei, H. Tang, and M.J. Berry II. Low error discrimination using a correlated population code. *Journal of neurophysiology*, 108(4):1069–1088, August 2012.

[33] Roman Shusterman, Matthew C Smear, Alexei A Koulakov, and Dmitry Rinberg. Precise olfactory responses tile the sniff cycle. *Nature neuroscience*, 14(8):1039–1044, 2011.

[34] Matthew Smear, Roman Shusterman, Rodney O'Connor, Thomas Bozza, and Dmitry Rinberg. Perception of sniff phase in mouse olfaction. *Nature*, 479(7373):397–400, 2011.

[35] S. Thorpe, A. Delorme, and R. VanRullen. Spike based strategies for rapid processing. *Neural Networks*, 14:715–726, 2001.

[36] S. Thorpe, D. Fize, and C. Marlot. Speed of processing in the human visual system. *Nature*, 381:520–522, 1996.

[37] M. van Wyk, W.R. Taylor, and D.I. Vaney. Local edge detectors: A substrate for fine spatial vision at low temporal frequencies in rabbit retina. *Journal of Neuroscience*, 26(51):13250, 2006.

[38] Rufin VanRullen, Rudy Guyonneau, and Simon J Thorpe. Spike times make sense. *Trends in Neurosciences*, 28(1):1–4, 2005.

[39] D.K. Warland, P. Reinagel, and M. Meister. Decoding visual information from a population of retinal ganglion cells. *J. Neurophysiol*, 78:2336–2350, 1997.

[40] Yifeng Zhang, In-Jung Kim, Joshua R Sanes, and Markus Meister. The most numerous ganglion cell type of the mouse retina is a selective feature detector. *Proceedings of the National Academy of Sciences*, 109(36):E2391–E2398, 2012.

Contents

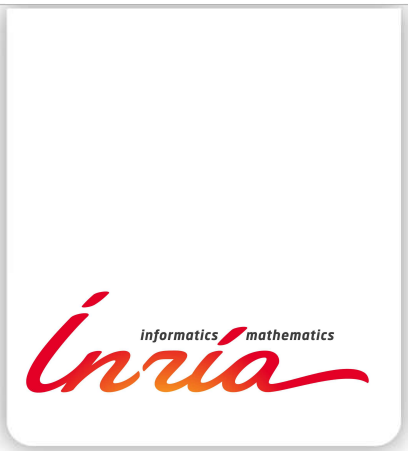

RESEARCH CENTRE
SOPHIA ANTIPOLIS – MÉDITERRANÉE

2004 route des Lucioles - BP 93
06902 Sophia Antipolis Cedex

Publisher
Inria
Domaine de Voluceau - Rocquencourt
BP 105 - 78153 Le Chesnay Cedex
inria.fr

ISSN 0249-6399